Contents lists available at ScienceDirect

Heliyon

journal homepage: www.cell.com/heliyon

Research article

Ethanol-free antisolvent crystallization of glycine by liquefied dimethyl ether

Hideki Kanda [a,b,c,*], Tsubasa Katsube [a], Rintaro Hoshino [a], Mitsuhiro Kishino [d], Wahyudiono [a], Motonobu Goto [a]

[a] *Department of Materials Process Engineering, Nagoya University, Furocho, Chikusa, Nagoya, 464-8603, Japan*
[b] *PRESTO, Japan Science and Technology Agency, 4-1-8 Honcho, Kawaguchi, Saitama, 332-0012, Japan*
[c] *SATREPS, Japan Science and Technology Agency, 4-1-8 Honcho, Kawaguchi, Saitama, 332-0012, Japan*
[d] *Research Institute for Bioscience Products & Fine Chemicals, Ajinomoto Co., Inc., 1-1 Suzukicho, Kawasakiku, Kawasaki 210-8681, Japan*

A B S T R A C T

Liquefied dimethyl ether (DME) was employed as an antisolvent to crystallize glycine from its aqueous solution. The proposed method can be performed at 20–25 °C and has the potential to reduce the energy consumption of drying or crystallizing using ethanol. α-Glycine crystals were successfully obtained from glycine aqueous solutions by mixing in liquefied DME, which was easily removed from the crystals by decompression. Contact with a liquefied DME/water mixture and small γ-glycine crystals resulted in the α-glycine converting to γ-glycine. This was only observed for saturated glycine solutions. We speculated that this conversion occurs via a solution-mediated transition. Pure liquefied DME is not capable of promoting solvent-mediated transitions, so saturated glycine solutions treated with the pure antisolvent can give α-glycine as the sole product.

1. Introduction

Crystallization is a significant industrial process that is widely used in pharmaceutical, food, and fine-chemical industries for separating and/or purifying products from reaction solutions. During crystallization processes, the physical properties of the final product, such as its chemical purity, crystal size distribution, and morphology, are changed by several factors, including temperature reduction and the antisolvent/solution ratio. In pharmaceutical industries these properties affect the bioavailability of materials [1, 2].

Glycine is non-toxic and is highly water soluble. It has been generally used as a bulking agent for freeze-dried protein formulations, where it inhibited the aggregation of certain proteins upon freezing [3, 4]. Dry glycine powder, from spray-drying, has also been investigated for applications in pulmonary delivery [5]. When spray-drying glycine, the latent heat and boiling point of water are increased with decreasing of water content in glycine solution. Therefore, glycine is a product typically obtained by antisolvent crystallization. The energy consumed by ethanol antisolvent crystallization is lower than that consumed by the spray-drying processes. However, because of the high boiling point of

ethanol and the azeotropic phenomenon (Figure 1 (a)), ethanol antisolvent crystallization requires high temperatures to separate the ethanol from water after crystallization. Electric furnaces or boiler are employed to achieve this high temperature; however, it is necessary to consume electricity or burn fossil fuels for them to operate. Therefore, an antisolvent that does not require a high temperature heat source is desirable. In addition, ethanol is contraindicated in various religions. To cope with such diversity, it is desirable to develop an antisolvent crystallization method that does not involve ethanol. Herein, we propose liquid dimethyl ether (DME) as an alternative antisolvent for glycine crystallization.

The normal boiling point of DME is $-24.8\,^{\circ}$C; thus, it is gaseous under standard conditions with a saturated vapor pressure of 0.59 MPa at 25 °C [6]. Liquefied DME is partially miscible with water, where the saturated water concentration in liquefied DME is approximately 7.5 wt.% at 25 °C [7, 8, 9]. Based on these characteristics, several groups have carried out dewatering processes using DME, as well as extracted several organic components from lignite, soil, plants, and biomass using DME as the solvent medium [10, 11, 12, 13, 14, 15, 16, 17, 18, 19, 20, 21, 22, 23, 24, 25]. This technique simultaneously extracted the organic components

---

and water from wet materials. Specifically, lipids extracted from wet microalgae by liquefied DME consisted mainly of C, H, and O, while the N content remained in the residue [21, 25]. Because microalgae contain numerous amino acids and proteins, these results imply that liquefied DME can be employed as an antisolvent for isolating amino acids and proteins.

There are a few studies that employ DME to separate proteins and lipids. Catchpole et al. utilized the DME as an effective antisolvent for proteins in an aqueous solution [16, 19]. This technique was applied to fresh and reconstituted egg yolks and on selected dairy by-product streams, where the lipids were removed from these materials using liquefied DME. The results showed that amino acids did not dissolve in the liquefied DME, thus cementing it as a potential antisolvent for their crystallization.

The low boiling point of DME negates the need for high-temperature heat sources. This was supported by an extraction study that showed that methods employing liquefied DME required substantially less energy consumption than those using other solvents [25]. Antisolvent crystallization by liquefied DME is shown in Figure 1(b). DME has been approved as a safe extraction solvent for the production of foodstuffs and food ingredients [26, 27]. Moreover, it exhibits resistance to autoxidation, unlike other alkyl ethers [28]. Therefore, there are no safety concerns associated with the use of liquefied DME for glycine crystallization.

In this study, the efficacy of glycine crystallization using liquefied DME was evaluated. The morphologies, sizes, and crystal structures of the glycine crystals obtained under various conditions were examined.

2. Materials and methods

2.1. Samples and chemicals

Purified DME (supplied as a propellant filled in a spray-work air can 420D, Tamiya, Inc., Shizuoka, Japan) was used as the antisolvent. Distilled water obtained from a water distillation apparatus (Auto still WS200, Yamato Scientific Co. LTD., Tokyo, Japan) was used as the solvent. Glycine (99.0%, Wako Pure Chemicals Industries Ltd, Osaka, Japan) was used as the solute. The concentration of the unsaturated glycine solution was 10.3 wt.% and that of the saturated solution was 20.2 wt.%. The glycine was completely dissolved in the unsaturated solution. The saturated glycine aqueous solution was filtered through a 0.65-μm filter (DVPP1300, Merck Millipore, MA, USA) to remove undissolved glycine crystals, but it was considered to contain glycine crystals <0.65 μm in size.

2.2. Experimental setup and procedure

Figure 2 shows the schematic diagram of the apparatus employed to conduct glycine crystallization by liquefied DME. The main apparatus consisted of an HPLC pump (880-PU; Jasco, Tokyo, Japan) for feeding the glycine solution, a crystallization reactor made of pressure resistance
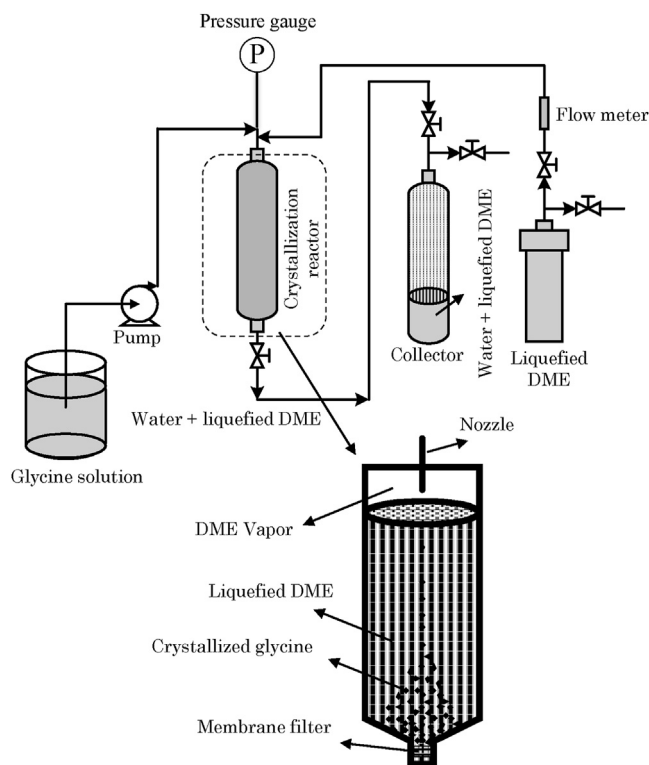

Figure 2. Glycine crystallization equipment using liquefied DME.

glass covered by polycarbonate (upper half of HPG-96-3 and lower half of HPG-96-5 were cut and combined; volume: 96 mL; inner diameter: 27 mm; Taiatsu Techno Corp., Saitama, Japan), a DME supply tank made of SS 316 (TVS-1-100; volume: 100 mL; Taiatsu Techno Corp., Saitama, Japan) that was equipped with a needle valve, and a collector made of pressure resistance glass covered by polycarbonate (HPG-96-3; volume: 96 mL; Taiatsu Techno Corp., Saitama, Japan). A 0.65-μm filter (DVPP1300, Merck Millipore) was placed at the bottom of the crystallization reactor. The flow rate of liquefied DME was controlled by a flow meter (P-100 customized for liquefied DME, Tokyo Keiso Co., Ltd, Tokyo, Japan). These were connected via 1/16-inch SS 316 tubes.

Liquefied DME in the DME supply tank was maintained at $35 \pm 1\ ^\circ$C in a water bath with a saturated vapor pressure of 0.78 ± 0.02 MPa. This pressure was measured by a pressure gauge connected to the DME supply tank. The inside of the DME supply tank was in a state of gas-liquid coexistence, and the vapor pressure was equal to the saturation vapor pressure. The liquefied DME was flowed into the crystallization reactor by the pressure difference between the DME supply tank and crystallization reactor. Infrared, non-contact thermometers detected that the temperature of the liquefied DME dropped rapidly, by approximately 25
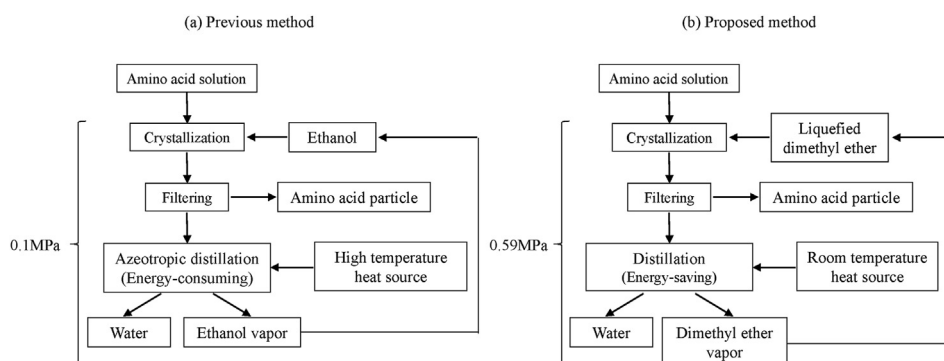

Figure 1. Procedure for antisolvent crystallization using (a) a previous method and (b) the proposed method.

°C, as it passed through the SS 316 tubing at the crystallization reactor inlet. The internal pressure of the crystallization reactor was measured by a pressure gauge connected to the crystallization reactor, which was 0.59 MPa.

First, 83 mL of liquefied DME was charged into the crystallization reactor. The glycine solutions were then injected from a nozzle to the surface of liquefied DME for 1 min. The flow rate of the glycine solution was 5 mL/min, which was controlled by the HPLC pump. The inside diameter of the nozzle was 0.25 mm and the initial distance between the nozzle tip and the surface of liquefied DME was 23 mm. During the injection of the glycine solution, the liquefied DME surface level was elevated.

After 5 mL of the unsaturated glycine solution (water amount was 4.49 g) was mixed with 83 mL (54.9 g; the density of liquefied DME at 25 °C is 0.661 g/mL) of liquefied DME, the water concentration of liquefied DME became 8.2 wt.% based on the liquefied DME weight. Liquefied DME at 25 °C is considered water-saturated when the water concentration is 7.5 wt.% [8]; therefore, the liquefied DME here is water-saturated. As a result, the undissolved water is separated into the lower layer of the liquefied DME. Also, when using the saturated glycine solution, the liquefied DME is saturated with water.

The crystalized glycine powders were trapped by the filter at bottom of the crystallization reactor and possessed very high-water content due to the water-saturated liquefied DME. To remove this water, additional liquefied DME charged in through the top of the crystallization reactor while the liquefied DME containing water was discharged from the bottom. The bottom of the crystallization reactor was equipped with a hand-operated pressure relief valve, whose opening was adjusted so as to keep the level of the liquefied DME constant while the additional liquefied DME was being charged. The liquefied DME flow rate was 20 ± 3 mL/min. Liquefied DME in the collector tank was decompressed and evaporated at 20–25 °C by opening a valve connected to the collector tank.

After feeding various amounts of liquefied DME, the remaining liquefied DME in the crystallization reactor was removed to the collector. Glycine powder was obtained from the filter at the bottom of the crystallization reactor and then analyzed.

2.3. Characterization

The water content of the glycine powders was measured using a moisture meter (Frontlab, AS ONE Corporation, Tokyo, Japan). When the weight reached a certain level by heating to 107 °C, the water content was determined from the difference from the initial weight.

Residual DME vapor in the glycine powder was detected by a gas chromatography/mass spectrometry (GC/MS) head space system according [29]. The glycine powder (0.50 g) was place in a 10 mL headspace vial. The GC/MS analysis was carried out using an Agilent 7890B GC system connected to an Agilent 5977A mass spectrometer using a cyanopropyl capillary column (VF0624MS; 60 m × 0.32 mm (i.d.) × 1.8 μm, Agilent Technologies Tokyo Ltd., Hachioji, Japan). An Agilent 7697A headspace sampler was also connected. The heating temperature of the head space was 50 °C and the vial equilibration time was set at 10 min. The oven temperature was initially set at 40 °C for 5 min and was then allowed to ramp up to 260 °C at a rate of 5 °C/min. The mass range was 29–450 m/z and the injector and interface temperatures were set at 150 and 240 °C, respectively.

The morphologies and sizes of the glycine powders were observed by scanning electron microscope (SEM) using a JSM-6390LV microscope (JEOL Ltd., Tokyo, Japan). The acceleration voltage was 1.0 kV.

X-ray diffraction (XRD) (RINT 2100/PC; 40 kV and 200 mA; Rigaku, Akishima, Japan) was used to confirm the crystal structure of glycine. It was equipped with a θ–θ wide-angle goniometer and scintillation detector and used Cu Kα radiation (λ = 1.5406 Å) with a scan rate of 2°/min, step size of 0.02, and a 2θ range of 10–50°.

A series of experiments, from crystallization by liquefied DME to analysis, was repeated three times with very similar analysis results.

3. Results and discussion

Unsaturated glycine solutions and saturated glycine solutions were sprayed into the liquefied DME in the crystallization reactor, where it was visually observed that glycine instantaneously crystallized from both the aqueous solutions.

In the glycine aqueous solution, water obstructs the growth of nascent glycine crystals, owing to the strong interactions between the OH_{water}–$O_{glycine}$ and $NH_{glycine}$–O_{water} hydrogen bonds [30]. The successful crystallization by liquefied DME implies the breakage of hydrogen bonds between the water and glycine molecules.

First, the results of the unsaturated glycine aqueous solution are discussed. After the injection of the unsaturated glycine solution into the liquefied DME, the pressure inside the crystallization reactor was reduced to atmospheric pressure, and the glycine powder remaining in the crystallization reactor was taken out. The obtained glycine powder had a water content of 24.1 ± 3 wt.%. Removal of this water from the glycine powder is crucial. Therefore, after the injection of the glycine unsaturated solution, without lowering the pressure in the crystallization reactor, pure liquefied DME was added to the crystallization reactor while an equal amount of water-containing liquefied DME was discharged from the bottom of the crystallization reactor. As a result, the amount of water in the crystallization reactor decreased.

After allowing 126 mL of additional liquefied DME to flow through the crystallization reactor, the pressure inside it was reduced and all the solution was discharged. The glycine crystal was subsequently removed from the crystallization reactor. The water content of glycine crystal was below the detection limit of 0.1%, which demonstrated the successful crystallization of glycine from the aqueous solutions and the removal of the water trapped within the crystals, simultaneously. We observed no ethereal odor in the obtained glycine powders; head space GC/MS analysis detected no DME vapor. This shows that DME was easily removed from the glycine powders at 20–25 °C. This was also the case when the amount of additional DME that was added to remove the water was varied, and the saturated glycine solution was used. The non-retention of DME in glycine implies that DME interacts strongly with water and weakly with glycine, thus removing the DME and water molecules from the glycine crystals. Previous studies have shown that the evaporated DME gas can be recovered and re-liquefied and reused as pure liquefied DME in an extraction solvent [15, 17, 18]. This is due to the fact that the difference in vapor pressure between DME and water at 25–40 °C is very large. Therefore, the reuse of liquefied DME obtained by evaporation and liquefaction does not interfere with this method.

SEM images (Figure 3(a-c)) were taken of the glycine powders after various amounts of additional liquefied DME were added or not added after the initial injection of the unsaturated glycine solution. As shown in Figure 3(a), needle-like glycine powders were generated when no additional liquefied DME was added to remove water. The length of the crystallized glycine particles was approximately 200 μm Figure 3 (b and c) show that the shape of the glycine powders did not change when the water was removed by the additional liquefied DME. This crystalline form seen in all the images corresponds to α-glycine [31, 32, 33]. The crystallized glycine particles became shorter in length and were mixed with particles of several tens of micrometers in length. This suggests that the addition of new liquefied DME gave preference to the creation of new glycine particles over the growth of existing glycine particles when the glycine saturation solubility in the liquefied DME/water mixture was reduced. The crystal structure of the glycine powder was analyzed by powder XRD. As a pretreatment for XRD analysis, the glycine powder was completely dried by sealing it in a desiccator for 1 day at a relative humidity of 20 % and 20–25 °C. The XRD patterns of the powders treated and not treated with additional liquified DME both showed peaks corresponding to good crystallinity of α-glycine (Figure 4(a-c)) [33, 34, 35,
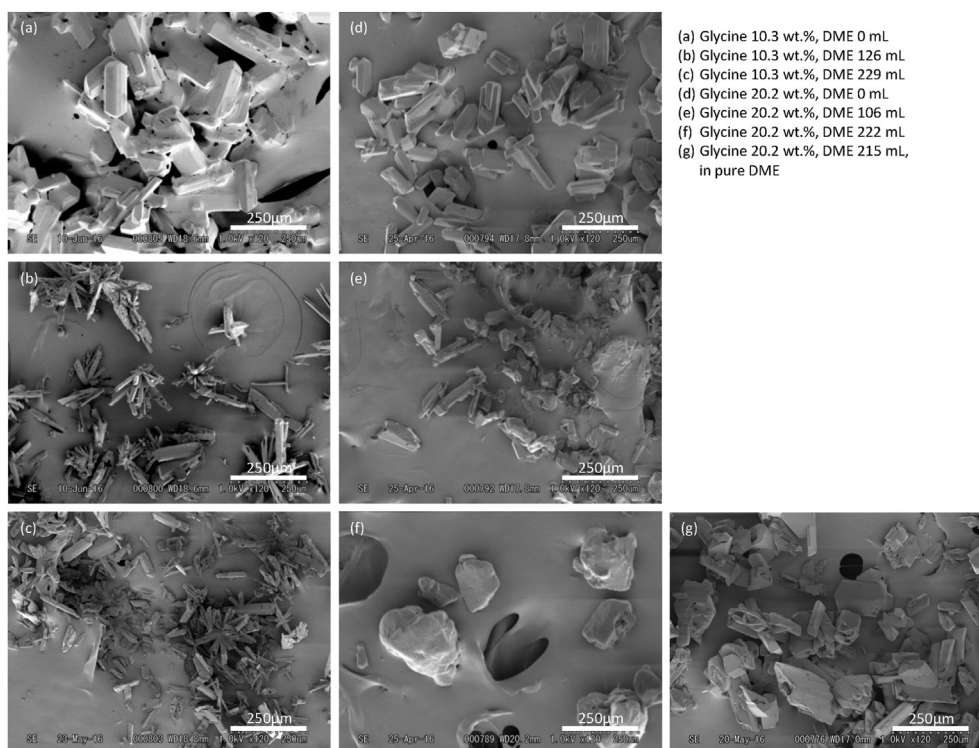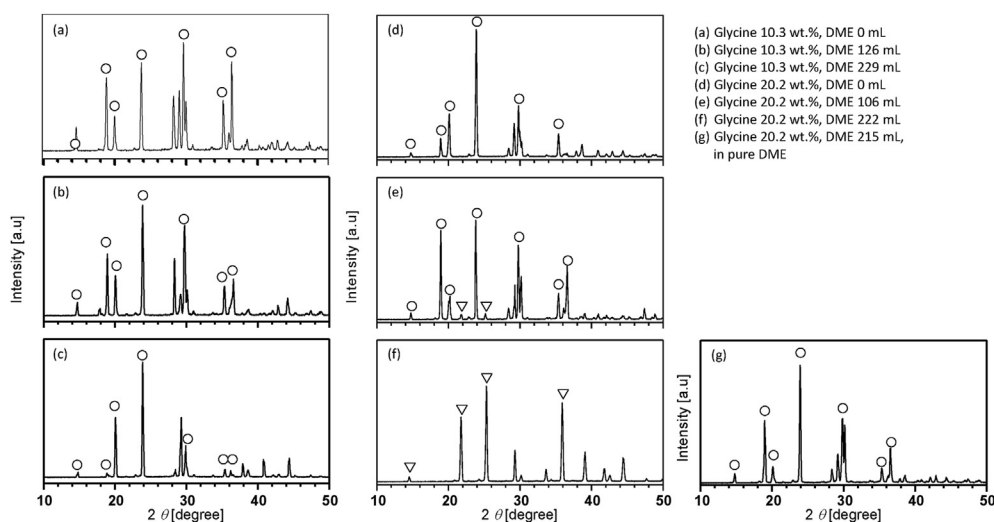
Figure 3. Scanning electron microscopy (SEM) images of glycine powders: (a) Unsaturated solution, no additional dimethyl ether (DME); (b) unsaturated solution, 126 mL of additional DME; (c) unsaturated solution, 229 mL of additional DME; (d) saturated solution, no additional DME; (e) saturated solution, 106 mL of additional DME; (f) saturated solution, 222 mL of additional DME; and (g) saturated solution and pure liquefied DME.

36]. The formation of the metastable α-glycine suggests that the solubility of glycine decreased very rapidly due to the swift dissolution of water from the glycine solution into the liquefied DME. When the solution is sufficiently supersaturated, Ostwald's step rule is known to give preference to crystalline forms with low surface energy, i.e., those with low thermodynamic stability [37]. This result with the appearance of the metastable phase, α-glycine, is consistent with Ostwald's step rule, since the spray of glycine solution into liquefied DME is able to reach supersaturation of glycine more rapidly than the addition of liquefied DME to glycine solution.

In general, the type of antisolvent and its concentration affects the polymorphs of crystals [38]. The saturated glycine solution was evaluated to examine if the concentration of the injected glycine solution had

any influence on crystallization. Upon injecting the saturated glycine solution, and without additional liquefied DME being added, a wet glycine powder was obtained with a water content of 31.1 $\pm$ 3 wt.%. Similar to what was seen with the unsaturated glycine solution, needle-like glycine powder was produced from the saturated glycine solution before the additional liquified DME was added (Figure 3 (d)). The length of the crystallized glycine particles was approximately 200 μm, similar to that of the unsaturated glycine solution. The XRD pattern confirmed that α-glycine was also present in this glycine powder (Figure 4 (d)). Water removal was then tested by adding 106 mL of additional liquefied DME after the injection of the saturated glycine solution, where the water content was reduced to below the detection limit of less than 0.1 wt.%. Even when the additional amount of liquefied DME

Figure 4. X-ray diffraction (XRD) patterns of glycine crystals obtained under several conditions. The open circles indicate α-glycine peaks and the open triangles represent γ-glycine peaks. (a) Unsaturated solution, no additional DME; (b) unsaturated solution, 126 mL of additional DME; (c) unsaturated solution, 229 mL of additional DME; (d) saturated solution, no additional DME; (e) saturated solution, 106 mL of additional DME; (f) saturated solution, 222 mL of additional DME; and (g) saturated solution and pure liquefied DME.

was increased to 106 mL, the glycine crystals remained needle-shaped (Figure 3(e)). The additional liquefied DME made the glycine particles smaller overall. However, in the XRD pattern shown in Figure 4(e), not only was α-glycine observed, but γ-glycine, the stable phase [33, 34, 35, 36], was also detected. When the amount of additional liquefied DME was increased to 222 mL, the crystal structure of glycine changed to become cube-like (Figure 3(f)) and the XRD pattern showed only γ-glycine (Figure 4(f)). These XRD patterns show that α-glycine converts to the more stable γ-glycine. The cubic glycine particles grew again to approximately 200–300 μm in size. This could be explained if a small amount of γ-glycine crystals were initially mixed in the saturated glycine solution.

In a previous study, the application of the inner seeding method to glycine has been investigated by Doki [39], in which glycine was crystallized by cooling of aqueous solution and α-glycine particles were added as seeds. In their cooling method, γ-glycine was crystallized when seed of α-glycine was not added. In contrast, the addition of α-glycine seed resulted in α-glycine crystallization by their cooling method. They showed that it is possible to crystallize glycine in the same crystalline form as the pre-existing seed. The present method differs from their cooling crystallization method, but the existence of seed has controlled the crystal form of glycine in a similar way.

To elucidate the mechanism of the α-glycine crystal transition to γ-glycine, we focused on solution-mediated transition. Here, a previous study has shown that the saturated solubility of γ-glycine in water and mixtures of water and poor solvents (methanol, ethanol, 2-propanol, and acetone) is around 5% lower than that of α-glycine [40]. The solution-mediated transition is due to this difference in solubility, which is detailed below. As crystallization progresses, the glycine supersaturated concentration in the aqueous solution decreases towards the saturated solubility. The glycine concentration first decreases to the saturated solubility of α-glycine, where the crystallization of α-glycine stops. However, since the saturated solubility of γ-glycine is even lower, if γ-glycine seeds are present at this point, the crystallization of γ-glycine proceeds. Since the glycine concentration is lower than the saturated solubility of α-glycine, also the glycine molecules dissolved from α-glycine into the aqueous solution are provided for the growth of γ-glycine crystals [40]. The occurrence of the solution-mediated transition is consistent with the SEM observation that the particles became smaller once and then larger again when additional DME was supplied.

In contrast, in the case of a pure poor solvent in which glycine is not soluble at all, the difference in solubility between α-glycine and γ-glycine is almost zero, so no solution-mediated transition occurs. Here, it was assumed that the same logic as for alcohol-based poor solvents holds for liquefied DME. In the case of this study, after injecting the glycine solution, the liquefied DME in the crystallization reactor was saturated with water. If glycine is slightly soluble in the liquefied DME/water mixture, then this mixture is capable of promoting solvent-mediated transitions.
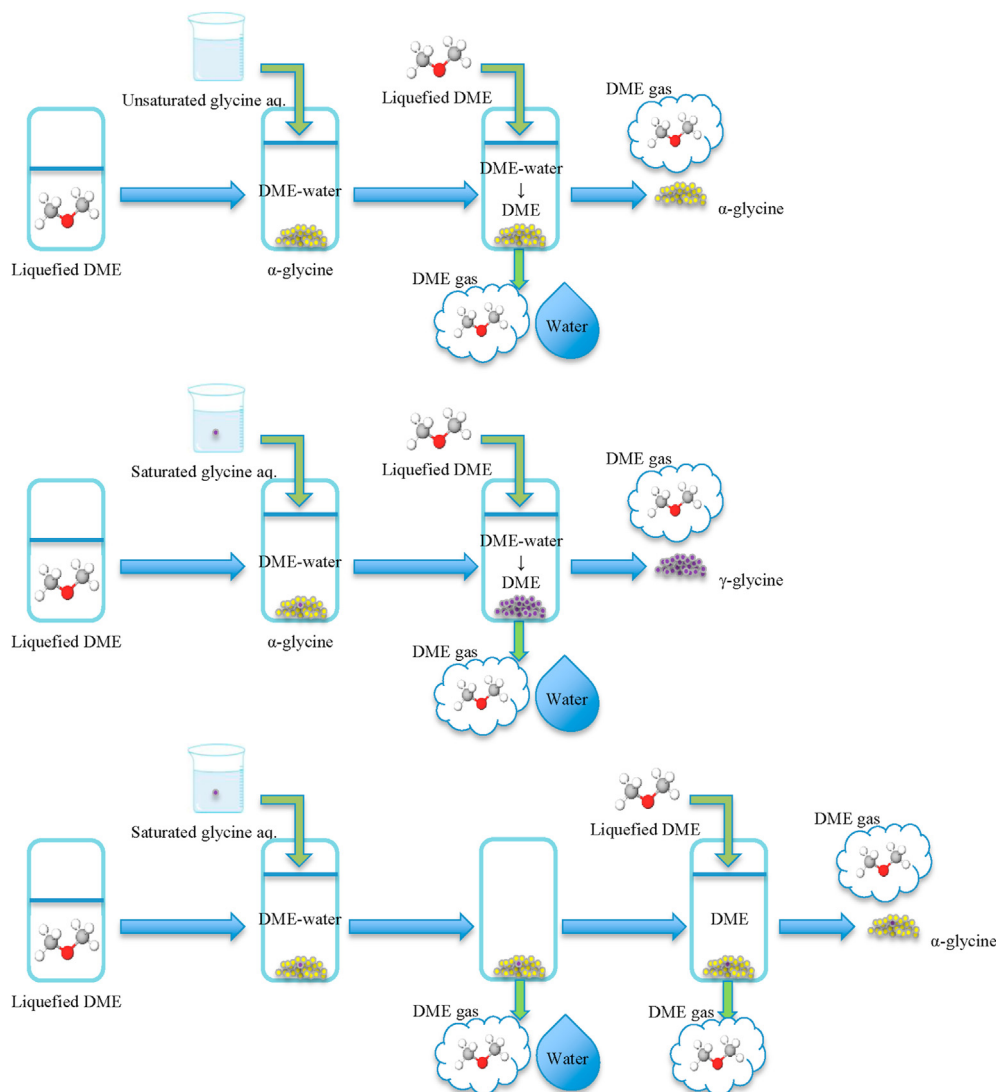

Figure 5. Relationship between glycine concentration and operation method and glycine crystal form.

An additional examination under pure liquified DME conditions was performed where the saturated glycine solution was injected into the liquefied DME within the crystallization reactor, all the water-saturated liquefied DME was removed, and then the crystallization reactor was refilled with pure liquefied DME. After then, additional pure liquefied DME was fed into the crystallization reactor at a flow rate of 20 ± 3 mL/min and removed from the bottom at the same rate. The level of liquefied DME within the reactor was maintained by manually adjusting the pressure relief valve. Under these pure liquefied DME conditions, α-glycine did not convert to γ-glycine when 215 mL of additional liquefied DME was added (Figure 3 (g) and Figure 4 (g)). These results demonstrated that the crystal transition occurred only in liquefied DME/water mixture, not in pure liquefied DME. Therefore, the glycine crystal form can be controlled by the concentration of the injected glycine solution, the amount of additional liquefied DME added, and by using either pure or water-saturated liquefied DME (See also Figure 5.).

For future scale-up of crystallization based on this method, it is important to stabilize the crystallization phenomenon by inner seeding method because the rapid increase of poor solvent may cause a blockage or crystallization at the contact point with the poor solvent. In a previous study by Doki [39], the seed amount of α-glycine was 33% of all crystallized glycine amounts, which is very high. In comparison, in the present study, the amount of γ-glycine seed was so low that it was expected, although the presence of γ-glycine seed in the saturated glycine solution is suspected. The amount of glycine seed needed for stable crystallization should be examined in the future scale up of liquefied DME crystallization method.

4. Conclusions

We proposed using liquefied DME as a new antisolvent for the crystallization of glycine from solutions. Glycine crystals were successfully obtained using liquefied DME, which was easily separated from the crystals at 20–25 °C. Liquefied DME has a low boiling point; therefore, this method has the potential to serve as an energy-saving crystallization process. α-Glycine was initially obtained by rapid and local supersaturation in the liquefied DME. Contact with a liquefied DME/water mixture and small γ-glycine crystals resulted in the α-glycine converting to γ-glycine. This was only observed for saturated glycine solutions. We speculated that this conversion occurs via a solution-mediated transition. Pure liquefied DME is not capable of promoting solvent-mediated transitions, so saturated glycine solutions treated with the pure antisolvent can give α-glycine as the sole product.

The method proposed here can potentially be applied to other water-soluble materials as an antisolvent crystallization method that does not use ethanol. We believe that our method is useful for reducing energy consumption and dealing with the religious repercussions surrounding the use of ethanol.

Declarations

Author contribution statement

Hideki Kanda: Conceived and designed the experiments; Contributed reagents, materials, analysis tools or data; Wrote the paper.

Tsubasa Katsube, Rintaro Hoshino, Wahyudiono: Performed the experiments; Analyzed and interpreted the data.

Mitsuhiro Kishino: Conceived and designed the experiments.

Motonobu Goto: Contributed reagents, materials, analysis tools or data.

Funding statement

Competing interest statement

The authors declare no conflict of interest.

Additional information

No additional information is available for this paper.

References

[1] V. Liotta, V. Sabesan, Monitoring and feedback control of supersaturation using ATR-FTIR to produce an active pharmaceutical ingredient of a desired crystal size, Org. Process Res. Dev. 8 (2004) 488–494.
[2] N. Ghadipasha, J.A. Romagnoli, S. Tronci, R. Baratti, On-line control of crystal properties in nonisothermal antisolvent crystallization, AIChE J. 61 (2015) 2188–2201.
[3] M.J. Akers, N. Milton, S.R. Byrm, S.L. Nail, Glycine crystallization during freezing: the effects of salt form, pH, and ionic strength, Pharm. Res 12 (1995) 1457–1461 (N. Y.).
[4] N.W. Hsiao, Y. Chen, Y.C. Kuan, Y.C. Lee, S.K. Lee, H.H. Chan, C.H. Kao, Purification and characterization of an aspartic protease from the Rhizopus oryzae protease extract, Peptidase R, Electron. J. Biotechnol. 17 (2014) 89–94.
[5] A. Nokhodchi, G.P. Martin, Pulmonary Drug Delivery Advances and Challenges, John Wiley & Sons, United Kingdom, 2015, p. 45.
[6] J. Wu, Y. Zhou, E.W. Lemmon, An equation of state for the thermodynamic properties of dimethyl ether, J. Phys. Chem. Ref. Data 40 (2011), 023104.
[7] M.E. Pozo, W.B. Streett, Fluid phase equilibria for the system dimethyl ether/water from 50 to 220 degree C and pressures to 50.9 MPa, J. Chem. Eng. Data 29 (1984) 324–329.
[8] H. Holldorff, H. Knapp, Binary vapor-liquid-liquid equilibrium of dimethyl ether-water and mutual solubilities of methyl chloride and water: experimental results and data reduction, Fluid Phase Equil. 44 (1988) 195–209.
[9] S. Tallon, K. Fenton, The solubility of water in mixtures of dimethyl ether and carbon dioxide, Fluid Phase Equil. 298 (2010) 60–66.
[10] H. Kanda, H. Shirai, Method for Removing Water Contained in Solid Using Liquefied Material, Patent Number – WO2003/101579 A1, Japan, 3 Jun 2002.
[11] O.J. Catchpole, J.B. Grey, N.B. Perry, E.J. Burgess, W.A. Redmond, N.G. Porter, Extraction of chili, black pepper, and ginger with near-critical CO₂, propane, and dimethyl ether: analysis of the extracts by quantitative nuclear magnetic resonance, J. Agric. Food Chem. 51 (2003) 4853–4860.
[12] S. Sato, A. Matsumura, Extraction of phenol in water phase using liquefied dimethyl ether, J. Jpn. Petrol. Inst. 46 (2003) 375–378.
[13] H. Kanda, Method for Removing Oil Contained in Water-Containing Substance Using Liquefied Matter, Patent number – JP4542517 B2, Japan, 10 Mar 2006.
[14] O. Catchpole, J. Grey, A. Mackenzie, S. Tallon, Extraction of highly unsaturated lipids with liquid dimethyl ether, Patent number – WO2007/136281 A1, New Zealand, 24 May 2006.
[15] H. Kanda, Super energy-saving dewatering method for high specific surface area fuels by using dimethyl ether, Adsorpt. Sci. Technol. 26 (2008) 345–349.
[16] O.J. Catchpole, S.J. Tallon, J.B. Grey, K. Fletche, A.J. Fletcher, Extraction of lipids from a specialist dairy stream, J. Supercrit. Fluids 45 (2008) 314–321.
[17] H. Kanda, H. Makino, Clean up process for oil-polluted materials by using liquefied DME, J. Environ. Eng. (JSME) 4 (2009) 356–361.
[18] K. Oshita, M. Takaoka, S. Kitade, K. Takeda, H. Kanda, H. Makino, T. Matsumoto, S. Morisawa, Extraction of PCBs and water from river sediment using liquefied dimethyl ether as an extractant, Chemosphere 78 (2010) 1148–1154.
[19] O. Catchpole, J. Ryan, Y. Zhu, K. Fenton, J. Grey, M. Vyssotski, A. MacKenzie, E. Nekrasov, K. Mitchell, Extraction of lipids from fermentation biomass using near-critical dimethylether, J. Supercrit. Fluids 53 (2010) 34–41.
[20] K. Oshita, M. Takaoka, Y. Nakajima, S. Morisawa, H. Kanda, H. Makino, N. Takeda, Sewage sludge dewatering process using liquefied dimethyl ether as solid fuel, Dry. Technol. 29 (2011) 624–632.
[21] P. Boonnoun, Y. Kurita, Y. Kamo, S. Machmudah, Y. Okita, E. Ohashi, H. Kanda, M. Goto, Wet extraction of lipids and astaxanthin from Haematococcus pluvialis by liquefied dimethyl ether, J. Nutr. Food Sci. 4 (2014) 305.
[22] P. Li, H. Kanda, H. Makino, Simultaneous production of bio-solid fuel and bio-crude from vegetal biomass using liquefied dimethyl ether, Fuel 116 (2014) 370–376.
[23] K. Sakuragi, P. Li, N. Aoki, M. Otaka, H. Makino, Oil recovery from wet Euglena gracilis by shaking with liquefied dimethyl ether, Fuel Process. Technol. 148 (2016) 184–187.
[24] Y. Hara, A. Kikuchi, A. Noriyasu, H. Furukawa, H. Takaichi, R. Inokuchi, F. Bouteau, S. Chin, X. Li, S. Nishihama, K. Yoshizuka, T. Kawano, Extraction of oil from rice bran by batch of liquefied low temperature dimethyl ether, Solvent Extr. Res. Dev. Jpn. 23 (2016) 87–99.
[25] H. Kanda, P. Li, M. Goto, H. Makino, Energy-saving lipid extraction from wet Euglena gracilis by low boiling point solvent dimethyl ether, Energies 8 (2015) 610–620.
[26] Panel on Food Contact Materials, Flavourings Enzymes, Processing Aids, Scientific Opinion on the safety of use of dimethyl ether as an extraction solvent under the

intended conditions of use and the proposed maximum residual limits, EFSA J 13 (2015) 4174.

[27] V. Varlet, F. Smith, M. Augsburger, New trends in the kitchen: propellants assessment of edible food aerosol sprays used on food, Food Chem. 142 (2014) 311–317.

[28] M. Naito, C. Radcliffe, Y. Wada, T. Hoshino, X. Liu, M. Arai, M. Tamura, A comparative study on the autoxidation of dimethyl ether (DME) comparison with diethyl ether (DEE) and diisopropyl ether (DIPE), J. Loss Prevent. Proc. 18 (2005) 469–473.

[29] R. Hoshino, M. Ogawa, K. Murakami, Wahyudiono, H. Kanda, M. Goto, Extraction of lipids from wet *Arthrospira platensis* by liquefied dimethyl ether, *Solvent Extr*, Res. Dev. J. 24 (2017) 47–60.

[30] I. Weissbuch, V.Y. Torbeev, L. Leiserowitz, M. Lahav, Solvent effect on crystal polymorphism: why addition of methanol or ethanol to aqueous solutions induces the precipitation of the least stable β form of glycine, Angew. Chem. Int. Ed. 44 (2005) 3226–3229.

[31] E.S. Ferrari, R.J. Davey, W.I. Cross, A.L. Gillon, C.S. Towler, Crystallization in polymorphic systems: the solution-mediated transformation of α to γ glycine, Cryst. Growth Des. 3 (2003) 53–60.

[32] B.D. Hamilton, I. Weissbuch, M. Lahav, M.A. Hillmyer, M.D. Ward, Manipulating crystal orientation in nanoscale cylindrical pores by stereochemical inhibition, J. Am. Chem. Soc. 131 (2009) 2588–2596.

[33] D.I. Trauffer, A.K. Maassel, R.C. Snyder, Non-needlelike morphology of β-glycine particles formed from water solutions via monodisperse droplet evaporation, Cryst. Growth Des. 16 (2016) 1917–1922.

[34] X. Yang, X. Wang, C.B. Ching, Solubility of form a and form γ of glycine in aqueous solutions, J. Chem. Eng. Data 53 (2008) 1133–1137.

[35] Z. Liu, L. Zhong, P. Ying, Z. Feng, C. Li, Crystallization of metastable β glycine from gas phase via the sublimation of α or γ form in vacuum, Biophys. Chem. 132 (2008) 18–22.

[36] R. Ezhil-Vizhi, C. Yogambal, D. Rajan Babu, Influence of sodium formate in γ-glycine single crystals – synthesis, growth and characterization, Optik 126 (2015) 77–80.

[37] M. Matsumoto, Y. Wada, A. Oonaka, K. Onoe, Polymorph control of glycine by antisolvent crystallization using nitrogen minute-bubbles, J. Cryst. Growth 373 (2013) 73–77.

[38] D.M. Croker, D.M. Kelly, D.E. Horgan, B.K. Hodnett, S.E. Lawrence, H.A. Moynihan, Å.C. Rasmuson, Demonstrating the influence of solvent choice and crystallization conditions on phenacetin crystal habit and particle size distribution, Org. Process Res. Dev. 19 (2015) 1826–1836.

[39] N. Doki, M. Yokota, K. Kido, S. Sasaki, N. Kubota, Reliable and selective crystallization of the metastable α-form glycine by seeding, Cryst. Growth Des. 4 (2004) 103–107.

[40] A. Bouchard, G.W. Hofland, G.-J. Witkamp, Solubility of glycine polymorphs and recrystallization of β-glycine, J. Chem. Eng. Data 52 (2007) 1626–1629.